Supporting Information

An x-ray absorption and x-ray photoelectron spectroscopic study of arsenic mobilization during mackinawite (FeS) oxidation

Hoon Y. Jeong,[†] Young-Soo Han,[‡] and Kim F. Hayes*[,‡]

[†]Pohang Accelerator Laboratory, Pohang University of Science and Technology (POSTECH), Pohang, 790784, Korea.

[‡]Department of Civil and Environmental Engineering, University of Michigan, Ann Arbor, MI 48109, USA.

*Corresponding author: Kim F. Hayes

Department of Civil and Environmental Engineering, University of Michigan, Ann Arbor, MI 48109, USA. Phone number: 1-734-763-9661; fax: 1-734-763-2275; e-mail: ford@umich.edu.

Submitted to Environmental Science and Technology

Manuscript was prepared on August 25, 2009

Pages (including the cover page): 16

Number of tables: 4 (S1–S4)

Number of figures: 5 (S1–S5)

XAS analysis.

All XAS spectra were analyzed using SixPACK (1). Individual spectra were averaged, and the background x-ray absorbance was removed by a linear fit through the pre-edge region. The x-ray absorption near-edge structure (XANES) region of the spectrum (11,860–11,890 eV) was obtained by normalizing the fluorescence signal to the edge-jump height. The absorption edges (i.e., inflection energies) in the XANES spectra were determined to compare the oxidation state of arsenic between samples and reference compounds. Extended x-ray absorption fine structure (EXAFS) spectra were isolated by fitting a quadratic spline function above the edge. The EXAFS spectra were normalized using a Victoreen polynomial function and transformed from energy to momentum space (k-space) using an E_0 of 11,885 eV. The resultant EXAFS functions ($\chi(k)$) were weighted by k^3 to amplify the upper k-range, and Fourier-transformed to produce radial structural functions (RSF) in R space over a k range of 3.5–11.5 $Å^{-1}$. Structural parameters were determined by fitting the weighted EXAFS functions ($k^3\chi(k)$) using phase and amplitude functions derived from FEFF 8 (2). The amplitude-reduction factor ($S_o^2 = 0.92$) was optimized from the fitting of the reference spectra and constrained for all data analysis. Note that the Debye-Waller factors (σ^2) were fixed based on either the similarity of the sample spectra to known reference compounds or the optimization among the sample spectra in order to reduce the degree of freedom in the data fitting. Other parameters such as coordination number (N), interatomic distance (R), and energy shift (ΔE_0) were allowed to vary. The data fitting was optimized by minimizing the goodness of fit parameter (R_f). Errors estimates of the fitted parameters are typically R ±0.02 Å and N ±20% (3-5).

XPS analysis.

Raw spectra, after being smoothed, were fitted into a Shirley baseline and a Gaussian-Lorentzian peak shape. Arsenic-3*d* spectra were fitted with the doublets of As $3d_{5/2}$ and $3d_{3/2}$ peaks with a spin-orbit splitting of 0.70 eV. The As $3d_{3/2}$ peak was constrained to be 2/3 the area of the As $3d_{5/2}$ peak. The full width at half maximum (FWHM) of all peak components were constrained in the fit. The resultant peak positions (i.e., binding energies) of As $3d_{5/2}$ lines for reference compounds are summarized in Table S2. Using the binding energies observed for five reference compounds, the As speciation of unoxidized samples was further determined. For quantitative analysis, the standard error of each component's contribution to the overall XPS spectrum was determined using Monte-Carlo analysis (CasaXPS, Casa Software Ltd., UK). This program applies artificial noise to a spectrum and calculates an error matrix to give the variance of each fit based on the fitting constraints used.

Species considered and thermodynamic constants (K) used for equilibrium calculations.

Type I species (components)

e-, H_2O, H^+, AsO_3^{3-}, AsO_4^{3-}, Cl^-, Fe^{2+}, Fe^{3+}, Na^+, SO_4^{2-}, HS^-

Type II species (aqueous complexes)

default K in MINEQL+4.5 (ref 6)

$NaSO_4^-$, OH^-, $Fe(OH)_3^-$, $Fe(OH)_2^o$, $FeOH^+$, $FeOH^{2+}$, $Fe(OH)_2^+$, $Fe_2(OH)_2^{4+}$, $Fe(OH)_3^o$, $Fe(OH)_4^-$, $Fe_3(OH)_4^{5+}$, $HAsO_3^{2-}$, $H_3AsO_3^o$, $H_2AsO_3^-$, $H_4AsO_3^+$, $HAsO_4^{2-}$, $H_2AsO_4^-$,

H_3AsO_4, HSO_4^-, S^{2-}, H_2S^o, $FeCl^{2+}$, $FeCl_2^+$, $FeCl_3^o$, $FeCl^{2+}$, $FeSO_4^o$, $Fe(HS)_2^o$, $Fe(HS)_3^-$, $FeSO_4^+$, $Fe(SO_4)_2^-$

<u>modified or added K</u>

$AsO_3^{3-} + HS^- + 4H^+ = As(OH)_2SH^o + H_2O$ log K = 43.434 (ref 7)

$AsO_3^{3-} + HS^- + 3H^+ = As(OH)_2S^- + H_2O$ log K = 38.284 (ref 7)

$AsO_3^{3-} + 2HS^- + 3H^+ = As(OH)S_2^{2-} + 2H_2O$ log K = 43.344 (ref. 7)

$AsO_3^{3-} + 3HS^- + 4H^+ = AsS_3H^{2-} + 3H_2O$ log K = 55.124 (ref 7)

$AsO_3^{3-} + 3HS^- + 3H^+ = AsS_3^{3-} + 3H_2O$ log K = 47.234 (ref 7)

$AsO_3^{3-} + 4HS^- + 6H^+ = As(SH)_4^- + 3H_2O$ log K = 71.284 (ref 7)

$AsO_3^{3-} + 2HS^- + 4H^+ = As(OH)S_2H^- + 2H_2O$ log K = 51.594 (ref 8)

$3AsO_3^{3-} + 6HS^- + 14H^+ = As_3S_6H_2^- + 9H_2O$ log K = 174.00 (ref 8)

Type V species (dissolved solids)

<u>default K in MINEQL+4.5 (ref 6)</u>

scorodite ($FeAsO_4 \cdot 2H_2O$), arsenolite (As_4O_6), As_2O_5, $Fe(OH)_2$, greigite (Fe_3S_4), mackinawite (FeS), goethite (α-FeOOH), lepidocrocite (γ-FeOOH), halite (NaCl), sulfur (S^0)

<u>modified or added K</u>

$2AsO_3^{3-} + 3HS^- + 9H^+ = As_2S_3(\text{disordered}) + 6H_2O$ log K = 114.288 (ref 9)

$AsO_3^{3-} + HS^- + 5H^+ + e^- = AsS(\text{realgar}) + 3H_2O$ log K = 54.281 (ref 10)

$AsO_3^{3-} + HS^- + Fe^{2+} + 5H^+ + 3e^- = FeAsS(\text{arsenopy.}) + 3H_2O$ log K = 43.40 (ref 11)

$AsO_3^{3-} + 6H^+ + 3e^- = As(0) + 3H_2O$ log K = 46.258 (ref 12)

Note: Since no thermodynamic data are available for disordered AsS, its stability region may be smaller than that estimated based on the formation constant for crystalline realgar.

Table S1. Dissolved species concentrations and mineralogy during FeS oxidation.

Oxidation time	Species	At pH 4.9	At pH 7.1	At pH 9.1
0 h	Fe (M)	1.53×10^{-3}M	8.03×10^{-6}M	7.72×10^{-6}M
	As (M)	2.70×10^{-8}M	2.11×10^{-6}M	7.05×10^{-5}M
	Sulfate (mg/L)	0.25	0.18	0.00
	Mineralogy	Mack[†]	Mack[†]	Mack[†]
1 h	Fe (M)	3.47×10^{-3}M	8.38×10^{-5}M	1.15×10^{-5}M
	As (M)	2.53×10^{-5}M	3.95×10^{-6}M	1.59×10^{-5}M
	Sulfate (mg/L)	0.60	0.54	0.10
	Mineralogy	Mack[†]	Mack+GR[†]	Mack[†]
2 h	Fe (M)	4.72×10^{-3}M	7.15×10^{-5}M	1.01×10^{-6}M
	As (M)	7.52×10^{-5}M	5.06×10^{-6}M	7.22×10^{-6}M
	Sulfate (mg/L)	0.62	0.94	0.11
	Mineralogy	Mack[†]	Mack+GR+Lepi[†]	Mack+Lepi[†]
4 h	Fe (M)	9.14×10^{-3}M	2.16×10^{-6}M	8.71×10^{-7}M
	As (M)	1.49×10^{-4}M	2.49×10^{-7}M	3.28×10^{-6}M
	Sulfate (mg/L)	0.63	1.93	0.11
	Mineralogy	GR[†]	GR+Lepi[†]	Mack+Lepi[†]
192 h	Fe (M)	1.24×10^{-3}M	1.79×10^{-6}M	6.33×10^{-7}M
	As (M)	ND[‡]	1.79×10^{-7}M	2.67×10^{-6}M
	Sulfate (mg/L)	0.68	1.94	0.54
	Mineralogy	Goe[†]	Lepi[†]	Lepi[†]

[†]Mack, GR, Goe, and Lepi represent mackinawite (FeS), green rusts, goethite (α-FeOOH), and lepidocrocite (γ-FeOOH), respectively.
[‡]ND means *not detected* at the detection limit of ~2.5×10^{-8}M.

Table S2. Characterization of reference compounds. Absorption edge positions and binding energies were obtained from XANES and XPS analyses, respectively.

References	Absorption edge positions	Binding energies (As $3d_{5/2}$)
As(0)	11,867.0 eV	41.6 eV
FeAsS	11,867.0 eV	
AsS	11,868.1 eV	42.84 eV
As_2S_3	11,869.0 eV	43.2 eV
$As(III)_{aq}$	11,870.9 eV	
$NaAsO_2$		43.6 eV
$As(V)_{aq}$	11,874.4 eV	
$Na_2HAO_4{\cdot}7H_2O$		44.47 eV

Table S3. EXAFS fit results and crystallographic data for reference compounds.

		EXAFS fit*			Crystallographic data		
	Pair	*N*	*R*(Å)	σ^2(Å^2)	*N*	*R*(Å)	Reference
As(0)	As-As	3.0	2.52	0.008†	3	2.50	ref 13
	As-As	1.5	3.12	0.0098†	3	3.13	
	As- As	4.1	3.75	0.014†	6	3.75	
	As- As	4.6	4.15	0.014†	6	4.12	
		ΔE_0 = -11.85 eV, R_f = 0.028					
FeAsS	As-S	1.3	2.34	0.035†	1	2.34	ref 14
	As-Fe	3.1	2.37	0.011†	3	2.36	
	As-As	3.0	3.06	0.013†	3	3.06-3.18	
	As-S				3	3.30	
	As-As	2.0	3.31	0.0092†	2	3.32	
	As-Fe	4.0	3.78	0.0091†	4	3.75	
	As-As	2.0	4.29	0.0065†	2	4.12	
		ΔE_0 = -8.88 eV, R_f = 0.038					
AsS	As-S	2.0	2.26	0.003†	2	2.24	ref 15
	As-As				1	2.57	
	As-As	0.41	3.50	0.006†	2.5	3.44-3.51	
	As-S				1	3.41-3.52	
		ΔE_0 = -9.80 eV, R_f = 0.061					
As_2S_3	As-S	3.0	2.28	0.0045†	3	2.24-2.31	ref 15
	As-As	0.37	3.54	0.006†	1	3.19	
	As-S				3	3.22-3.57	
	As-As				2.5	3.52-3.64	
		ΔE_0 = -7.75 eV, R_f = 0.047					
$As(III)_{aq}$	As(III)-O	3.0	1.76	0.0045†			
		ΔE_0 = -7.90 eV, R_f = 0.069					
$As(V)_{aq}$	As(V)-O	4.0	1.69	0.0025†			
		ΔE_0 = -5.01 eV, R_f = 0.024					

*The amplitude-reduction factor (S_o^2) was set at 0.92.
†The Debye-Waller factors (σ^2) were fixed during the numerical fit.

Table S4. EXAFS fit results for As(III)-reacted FeS during oxidation.*

		Samples at pH 4.9				Samples at pH 7.1				Samples at pH 9.1			
Oxidation	Shell	Pair	*N*	*R*(Å)	σ^2(Å^2)	Pair	*N*	*R*(Å)	σ^2(Å^2)	Pair	*N*	*R*(Å)	σ^2(Å^2)
0 h	1	As-S	1.9	2.25	0.003†	As-S	2.5	2.25	0.0055†	As-S	2.7	2.28	0.0055†
		As-As	1.7	2.52	0.008†	As-As	1.4	2.52	0.008†	As-As	0.92	2.52	0.008†
	2	As-As	1.8	3.51	0.006†	As-As	1.8	3.51	0.006†	As-As	0.77	3.56	0.006†
		ΔE_0 = -8.72 eV, R_f = 0.011				ΔE_0 = -9.03 eV, R_f = 0.026				ΔE_0 = -3.79 eV, R_f = 0.034			
1 h	1	As-S	2.3	2.26	0.003†	As(V)-O	2.4	1.69	0.0033†	As(V)-O	1.4	1.69	0.0033†
						As(III)-O	0.84	1.79	0.0037†	As(III)-O	2.2	1.79	0.0037†
	2	As-As	0.60	3.48	0.006†	As-Fe	0.27	2.92	0.0044†	As-Fe	0.33	2.95	0.0044†
						As-Fe	0.52	3.37	0.0048†	As-Fe	0.64	3.42	0.0048†
		ΔE_0 = -7.97 eV, R_f = 0.028				ΔE_0 = -11.24 eV, R_f = 0.051				ΔE_0 = -5.31 eV, R_f = 0.054			
2 h	1	As-S	2.6	2.27	0.003†	As(V)-O	3.3	1.69	0.0033†	As(V)-O	3.7	1.69	0.0033†
						As(III)-O	0.54	1.79	0.0037†	As(III)-O	0.28	1.79	0.0037†
	2	As-As	0.19	3.50	0.006†	As-Fe	0.30	2.95	0.0044†	As-Fe	0.41	2.90	0.0044†
						As-Fe	1.0	3.37	0.0048†	As-Fe	0.69	3.37	0.0048†
		ΔE_0 = -7.43 eV, R_f = 0.020				ΔE_0 = -12.00 eV, R_f = 0.044				ΔE_0 = -14.50 eV, R_f = 0.045			
4 h	1	As(V)-O	3.6	1.69	0.0033†	As(V)-O	3.8	1.69	0.0033†	As(V)-O	4.0	1.69	0.0033†
	2	As-Fe	0.40	2.90	0.0044†	As-Fe	0.36	2.94	0.0044†	As-Fe	0.35	2.90	0.0044†
		As-Fe	0.87	3.33	0.0048†	As-Fe	0.78	3.36	0.0048†	As-Fe	0.72	3.35	0.0048†
		ΔE_0 = -9.67 eV, R_f = 0.035				ΔE_0 = -12.60 eV, R_f = 0.044				ΔE_0 = -14.74 eV, R_f = 0.043			
192 h	1	As(V)-O	3.8	1.69	0.0033†	As(V)-O	3.9	1.69	0.0033†	As(V)-O	3.8	1.69	0.0033†
	2	As-Fe	0.37	2.88	0.0044†	As-Fe	0.32	2.92	0.0044†	As-Fe	0.36	2.91	0.0044†
		As-Fe	0.57	3.32	0.0048†	As-Fe	0.90	3.36	0.0048†	As-Fe	0.61	3.38	0.0048†
		ΔE_0 = -11.45 eV, R_f = 0.049				ΔE_0 = -10.86 eV, R_f = 0.041				ΔE_0 = -8.96 eV, R_f = 0.042			

*The amplitude-reduction factor (S_o^2) was set at 0.92. †The Debye-Waller factors (σ^2) were fixed during the numerical fit.
ΔE_0 and R_f indicate energy shift and goodness of the fit, respectively.

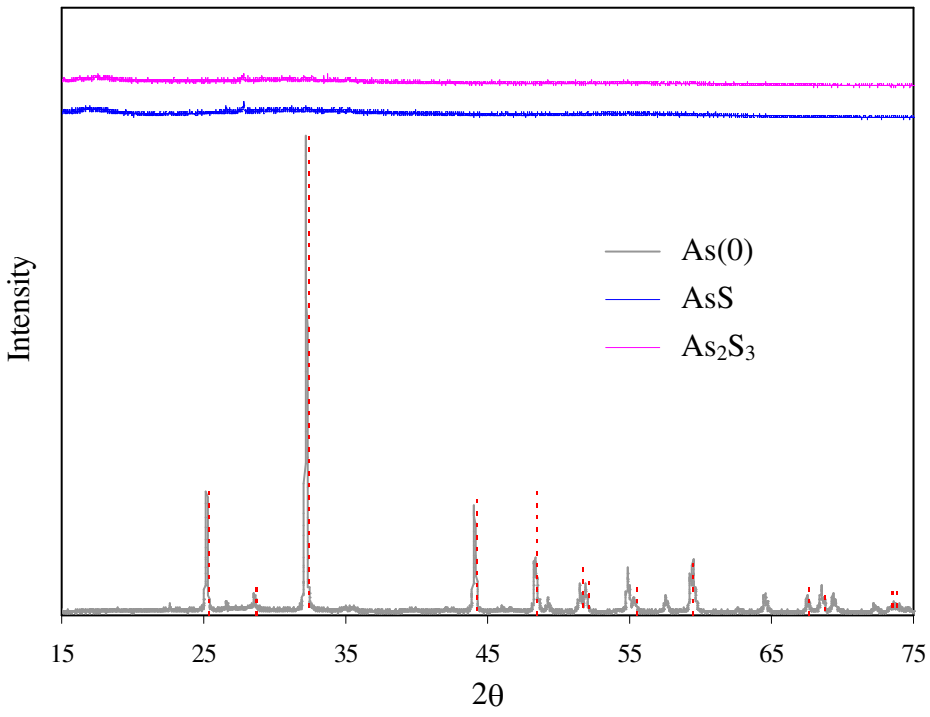

Figure S1. X-ray diffraction patterns for reference compounds with Cu-K_α radiation (40 kV and 100 mV). The diffraction pattern of As(0) matches that of PDF No. 00-005-0632, which is indicated by red dashed lines.

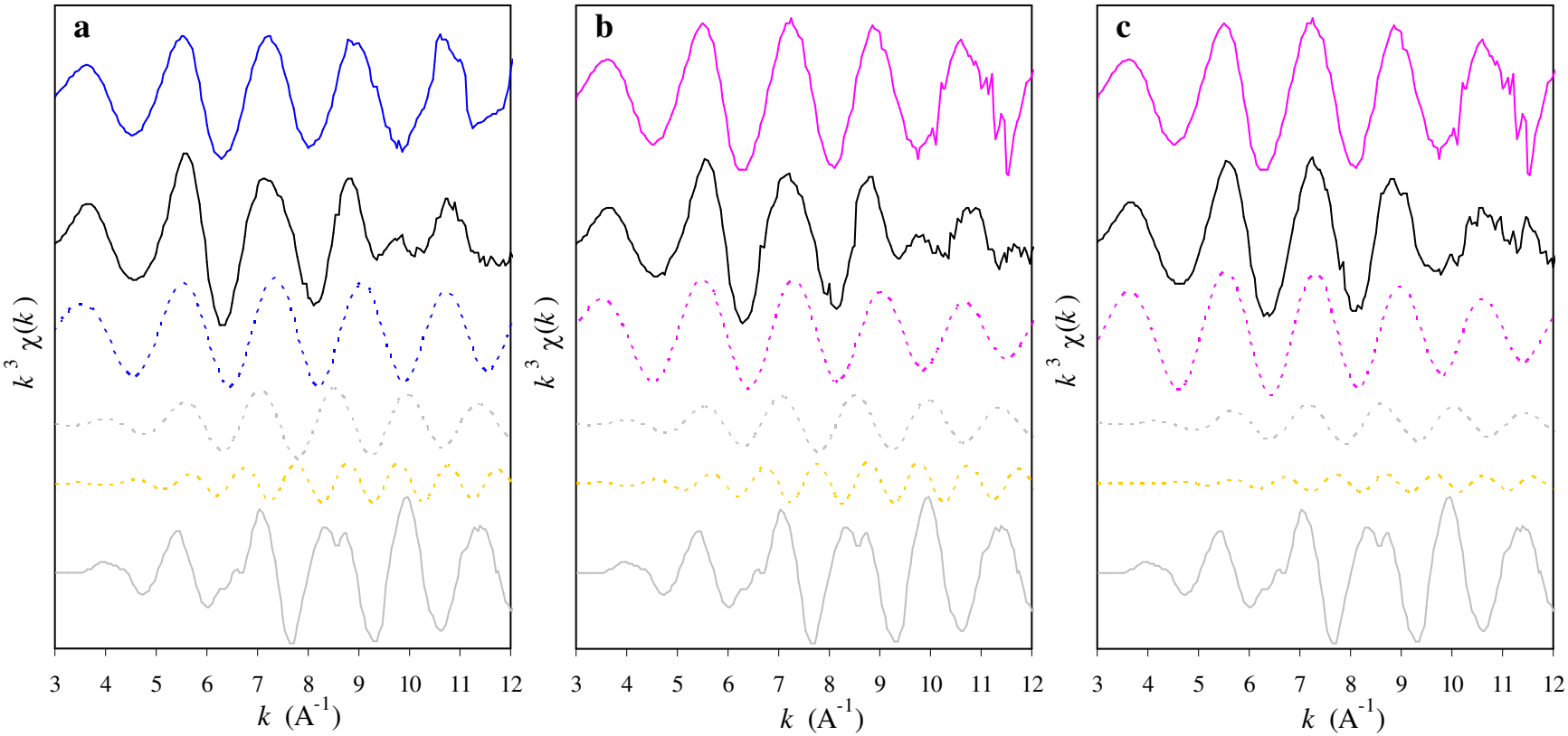

Figure S2. EXAFS component analysis of unoxidized samples at pH 4.9 (**a**), 7.1 (**b**), and 9.1 (**c**): the original sample spectra (black solid lines), As-S components (blue or pink dashed lines), As-As components at ~2.52 Å (grey dashed lines), and As-As components at ~3.5 Å (yellow dashed lines). The EXAFS spectra of As(0) (grey solid lines), disordered AsS (blue solid lines), and disordered As_2S_3 (pink solid lines) are included for comparison.

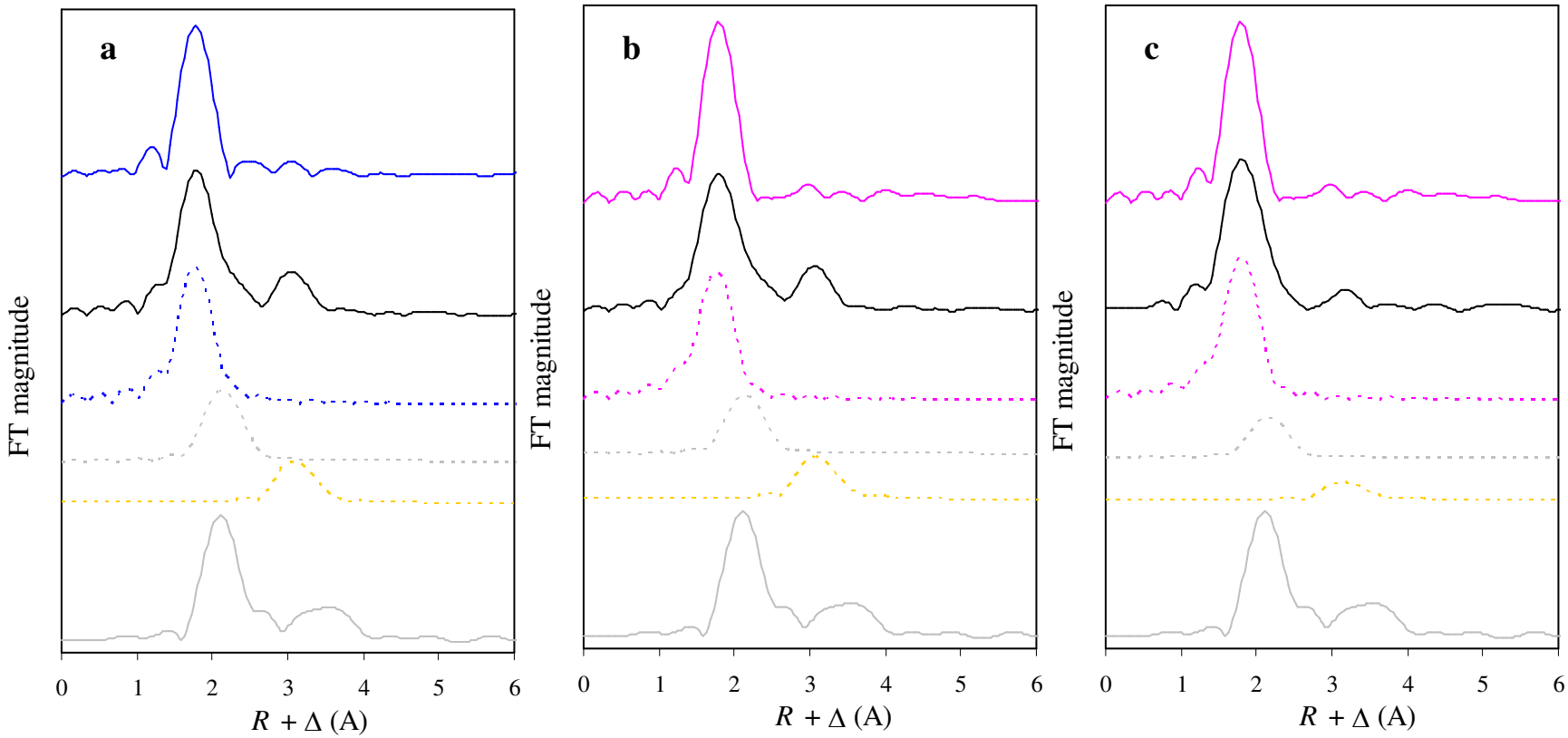

Figure S3. Fourier transform (FT) component analysis of unoxidized samples at pH 4.9 (**a**), 7.1 (**b**), and 9.1 (**c**): the original sample spectra (black solid lines), As-S components (blue or pink dashed lines), As-As components at ~2.52 Å (grey dashed lines), and As-As components at ~3.5 Å (yellow dashed lines). The FT spectra of As(0) (grey solid lines), disordered AsS (blue solid lines), and disordered As_2S_3 (pink solid lines) are included for comparison.

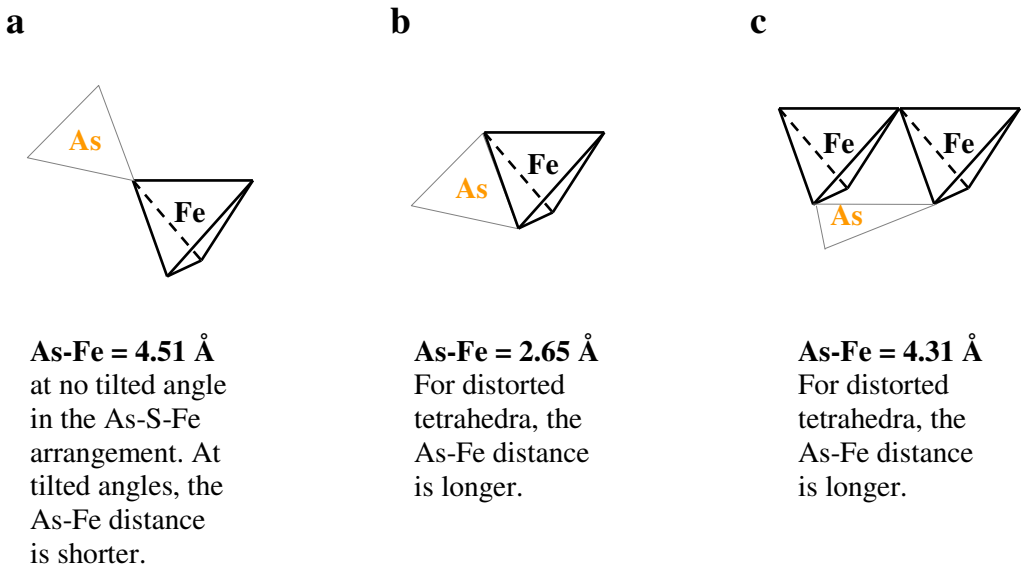

Figure S4. Geometries of thioarsenite surface complexes. Monodentate (single-corner sharing) (**a**), bidentate-mononuclear (edge sharing) (**b**), and bidentate-binuclear (double-corner sharing) (**c**) complexes with undistorted FeS_4 tetrahedra in mackinawite (FeS). In this figure, As-S = 2.27 Å (from the EXAFS analysis in this study), Fe-S in FeS = 2.24 Å (16), Fe-Fe in FeS = 2.60 Å (16), and S-S in FeS = 3.66 Å (16) were used to calculate the As-Fe bonding distances. The As-Fe distance observed in our EXAFS study (3.57–3.67 Å) is not consistent with the surface complexes of thioarsenites.

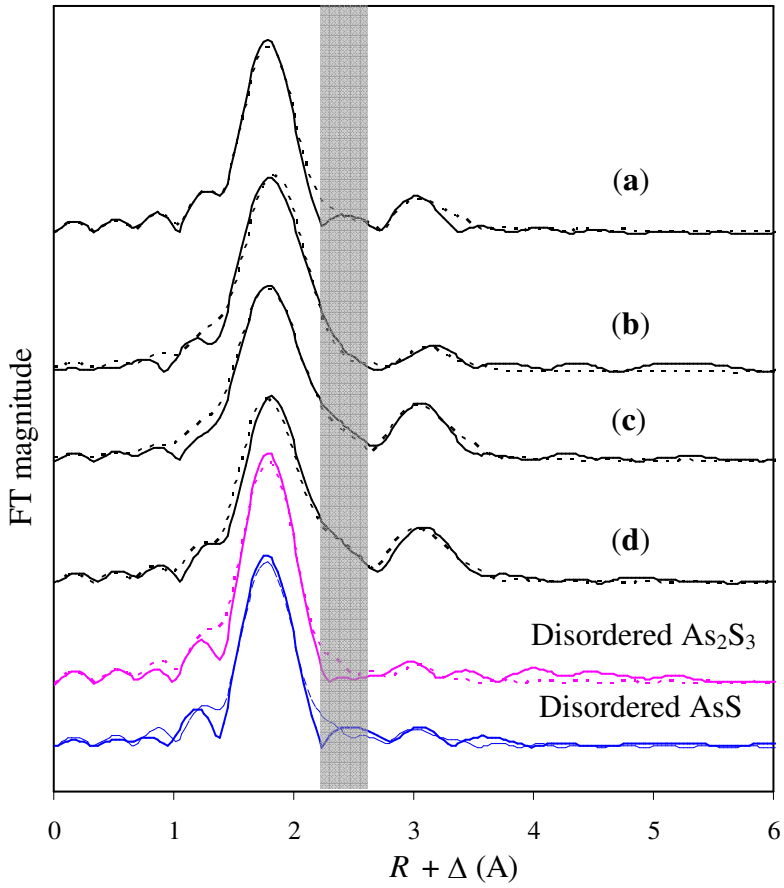

Figure S5. Fourier transforms of k^3-wieghted As-K edge EXAFS spectra for unoxidized samples: sample (**a**) (As(III)/[FeS] =2.3×10^{-3} mol/g at pH 5), sample (**b**) (As(III)/[FeS] =2×10^{-4} mol/g at pH 9.1 *from this study*), sample (**c**) (As(III)/[FeS] =2×10^{-4} mol/g at pH 7.1 *from this study*), and sample (**d**) (As(III)/[FeS] =2×10^{-4} mol/g at pH 4.9 *from this study*). Unlike samples (**b**)-(**d**), no significant right shoulder feature is observed for the first coordination shell of sample (**a**), whose absorption edge matches closely that of disordered AsS. Since electrons are needed for As(III) to form As(0) and AsS, the initially added As(III) acts as an oxidant. Thus, sample (**a**) due to the higher As(III)/[FeS] ration is at relatively more oxidized redox state, leading to formation of AsS only.

References cited in SI

1. Webb, S.M. *Sam's Interface for XAS Package (SixPACK)*; Stanford Synchrotron Radiation Laboratory: Menlo Park, CA, 2002.
2. Ankudinov, A.L.; Ravel, B.; Rehr, J.J.; Conradson, S.D. Real-space multiple-scattering calculation and interpretation of x-ray-absorption near-edge structure. *Phys. Rev. B* **1998**, *58*, 7565-7576.
3. Fendorf, S.; Eick, M.J.; Grossl, P.; Sparks, D.L. Arsenate and chromate retention mechanisms on goethite. 1. surface structure. *Environ. Sci. Tech*. **1997**, *31*, 315-320.
4. Manning, B.A.; Fendorf, S.E.; Goldberg, S. Surface structures and stability of arsenic(III) on goethite: spectroscopic evidence for inner-sphere complexes. *Environ. Sci. Tech*. **1998**, *32*, 2383-2388.
5. Manning, B.A.; Fendorf, S.E.; Bostick, B.; Suarez, D.L. Arsenic(III) oxidation and arsenic(V) adsorption reactions on synthetic birnessite. *Environ. Sci. Tech*. **2002**, *36*, 976-981.
6. Schecher, W.D.; McAvoy, D.C. *MINEQL+ 4.5*; Environmental Research Software: Hallowell, ME, 2001.
7. Wilkin, R.T.; Wallschläger, D.; Ford, R.G. Speciation of arsenic in sulfidic waters. *Geochem. Trans*. **2003**, *4*, 1-7.
8. Nordstrom, D.K.; Archer, D.G. In *Arsenic in Ground Water*; Welch, A.H., Stollenwerk, K.G., Eds.; Kluwer Academic Publishers: Boston, 2003; pp. 1-25.
9. Eary, L.E. The solubility of amorphous As_2S_3 from 25 to 90^{o}C. *Geochim. Cosmochim. Acta* **1992**, *56*, 2267-2280.
10. Barton, P.B. Thermochemical study of the system Fe-As-S. *Geochim. Cosmochim. Acta* **1969**, *33*, 841-857.

11. Wagman, D.D.; Evans, W.H.; Parker, V.B.; Schumm, R.H.; Halow, I.; Bailey, S.M.; Churney, K.L.; Nuttall, R.L. The NBS tables of chemical thermodynamic properties: selected values for inorganic and C1 and C2 organic substances in SI units. *J. Phys. Chem. Ref. Data* **1982**, *11*, 392.
12. Garrels, R.M.; Christ, C.L. *Solutions, Minerals, and Equilibria*; Haper & Row: New York, 1965.
13. Foster, A.L.; Brown, G.E.; Tingle, T.N.; Parks, G.A. Quantitative arsenic speciation in mine tailings using x-ray absorption spectroscopy. *Am. Mineral*. **1998**, *83*, 553-568.
14. Morimoto, N.; Clark, L.A. Arsenopyrite crystal-chemical relationships. *Am. Mineral*. **1961**, *46*, 1448-1469.
15. Mullen, D.J.E.; Nowacki, W. Refinement of the crystal structures of realgar, AsS and orpiment, As_2S_3. *Z. Kristallogr*. **1972**, *136*, 48-65.
16. Taylor, L.A.; Finger, L.W. Structural refinement and composition of mackinawite. *Carnegie Institution of Washington Geophysical Laboratory Annual Report* **1970**, *69*, 318-322.